SLAC-PUB-6277
UCD-93-20
SMU-HEP-93/09
RU-93-23
JUNE 1993
(T/E)

Guaranteed Detection of a Minimal Supersymmetric Model Higgs Boson at Hadron Supercolliders

J. Dai[a], J.F. Gunion[b] and R. Vega[c]

a) Dept. of Physics and Astronomy, Rutgers University, Piscataway, NJ 08855
b) Davis Institute for High Energy Physics, Dept. of Physics, U.C. Davis, Davis, CA 95616
c) Dept. of Physics, Southern Methodist University, Dallas, TX 75275
and
Stanford Linear Accelerator Center, Stanford, CA 94305

Abstract

We demonstrate that expected efficiencies and purities for b-tagging at SSC/LHC detectors should allow detection of at least one of the Higgs bosons of the Minimal Supersymmetric Model in $t\bar{t}$ Higgs production, with Higgs$\rightarrow b\bar{b}$ decay, over a substantial range of supersymmetric parameter space. In particular, with the addition of this mode to those previously considered, there is no region of supersymmetric parameter space for which *none* of the Higgs bosons of the model can be seen at the SSC/LHC.

1. Introduction and Procedure

Understanding the Higgs sector is a crucial mission for future high energy colliders such as the SSC and LHC. While it is quite certain that the SSC/LHC will be able to detect the Standard Model Higgs boson (ϕ^0), prospects for detection of the Higgs bosons of the Minimal Supersymmetric Model (MSSM) have appeared to be somewhat limited. In particular, in previous work[1,2] it became apparent that for $m_t \sim 150$ GeV there is a window of m_{A^0}–$\tan\beta$ parameter space, with $110 \lesssim m_{A^0} \lesssim 170$ GeV and $\tan\beta \gtrsim 10$, in which it could be that no MSSM Higgs boson would be seen either at LEP-II or at the SSC/LHC. (There is an even larger window where none could be seen just at the SSC/LHC.) For the former window to arise it is necessary that the squark mass be large enough ($\sim$ 1 TeV) that radiative corrections[3] to the mass of the lightest CP-even Higgs boson (h^0) are big, in particular, big enough that $Z^* \rightarrow Zh^0$ is not kinematically allowed at LEP-II when $\tan\beta$ is large and m_{A^0} takes on moderate to large values. In addition, the presence of this window of unobservability is based on the assumption that only the $\gamma\gamma$ and 4ℓ decay channels of the CP-even h^0 and H^0 Higgs bosons will lead to viable signals at the SSC/LHC,* and that detection of the

* Detection of the CP-odd A^0 in the $\gamma\gamma$ or 4ℓ decay channels is confined to the region of parameter space where $\tan\beta \lesssim 1$.

*Work supported by Department of Energy contract DE-AC03-76SF00515

$H^{\pm}$ will be possible only if $t \to H^+ b$ decays are kinematically allowed. Although it is not impossible that the portion of the window with very high $\tan\beta$ (where inclusive $b\bar{b}$ fusion yields enhanced Higgs boson cross sections) can be covered using the $\tau^+\tau^-$ decay modes of the H^0 and the A^0,[4] the precise parameter region over which it can be employed is a subject of continuing study.[5] In this letter, we demonstrate that a viable signal at the SSC/LHC for the primary decays $h^0 \to b\bar{b}$ or $H^0 \to b\bar{b}$ can be obtained in $t\bar{t}$ Higgs production over much of m_{A^0}–$\tan\beta$ parameter space (in particular, in the window in question).

In a previous paper,[6] we established that detection of the SM ϕ^0 in the $t\bar{t}b\bar{b}$ final state mode was, indeed, possible for a significant range of m_{ϕ^0}, provided $m_t \gtrsim 130 - 140$ GeV. The analysis of the present paper is based on the results of this previous work, to which we refer the reader for details. Several different detection scenarios were examined there. Here we consider only the case in which 3 b-quarks are required to be vertex tagged with efficiency of 30% and purity of 1% (after appropriate kinematic and vertex separation cuts). For this scenario, termed case I in Ref. 6, substantial peaks in the $b\bar{b}$ mass spectrum are visible for ϕ^0 masses in the region below about $110 - 120$ GeV. Of course, as argued in Ref. 6, it might be that the above assumptions regarding b-tagging efficiency and purity are too conservative. Detection of the MSSM Higgs bosons in the $t\bar{t}b\bar{b}$ final state mode would be even easier if, for instance, the b-tagging probability could be brought up to 40% while decreasing the misidentification probability to 0.5% over the stated kinematic range.

To convert the case I results for use in the MSSM, the following procedure is employed. First, we give the statistical significance of the $b\bar{b}$ mass peaks at Higgs masses of 80, 100, 120 and 140 GeV, for $m_t = 110$, 140 and 180 GeV, for $L = 10$ fb^{-1} at the SSC *assuming 100% $b\bar{b}$ branching ratio.*† The number of standard deviations obtained for $m_t = (110, 140, 180)$ is (4.0,5.0,10.2), (3.2,3.4,6.5), (2.7,3.1,3.9) and (2.1,2.4,3.1) at Higgs masses of 80, 100, 120 and 140 GeV, respectively. Interpolation/extrapolation is employed to obtain results for the top quark masses of 150 GeV and 200 GeV considered here, and for other values of Higgs mass. The appropriate result for the h^0 or H^0 is obtained by multiplying the number of standard deviations by the $b\bar{b}$ branching ratio of the h^0 or H^0 and by the square of the ratio of the h^0 or H^0 $t\bar{t}$ coupling to the $\phi^0 t\bar{t}$ coupling (to account for the difference in the $t\bar{t}$ Higgs production rates). Finally, if $t \to H^{\pm} b$ decays are allowed, the rate for the $t\bar{t}$ Higgs signal and for all the $t\bar{t}$-related backgrounds (see Ref. 6) must be appropriately reduced to account for the reduced trigger rate of an isolated lepton from one or two $t \to W^{\pm} b$ decays. Clearly, all these correction factors, not to mention the Higgs masses themselves, depend upon the supersymmetric model parameters, and in particular on m_{A^0} and $\tan\beta$.

To understand the results we shall obtain, it is useful to review some features of the MSSM Higgs sector.[7] First, recall that the h^0 and H^0 mass eigenstates are obtained by diagonalizing the CP-even mass-squared matrix. The result for $\tan\beta \gtrsim 2$ is a kind of level-crossing in which for low m_{A^0} the H^0 has a relatively constant mass value somewhat above m_Z. As m_{A^0} increases, m_{h^0} rises to 'meet' this constant value. For m_{A^0} values above the crossing point, m_{h^0} takes on a value which is a bit below or nearly the same (at large $\tan\beta$) as the constant value while m_{H^0} rises, becoming approximately degenerate with m_{A^0}. For

† Results for the LHC will not be given in this letter, but are substantially similar to those obtained for the SSC.

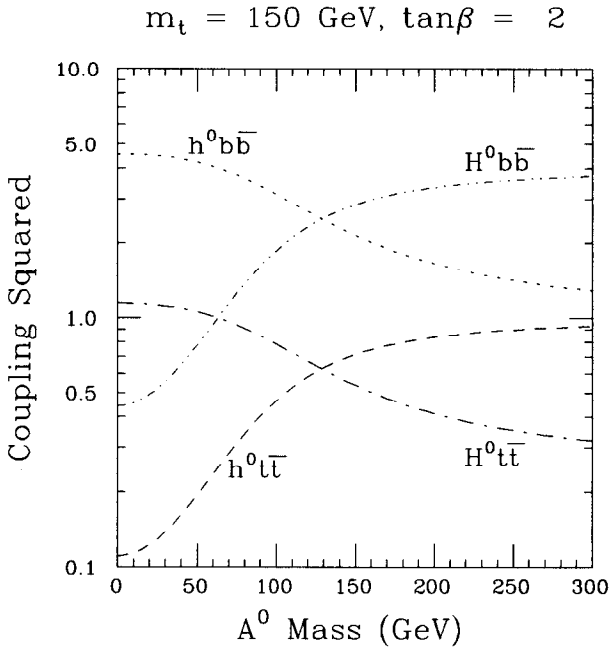

Figure 1: The ratios $g^2_{t\bar{t}h}/g^2_{t\bar{t}\phi^0}$ and $g^2_{b\bar{b}h}/g^2_{b\bar{b}\phi^0}$ ($h = h^0, H^0$) are plotted as a function of m_{A^0} at $\tan\beta = 2$ and $m_t = 150$ GeV. We have taken $M_{\tilde{t}} = 1$ TeV.

$m_t \sim 150$ GeV and $M_{\tilde{t}} \sim 1$ TeV, the constant mass value referred to above is in the vicinity of 100 GeV,‡ *i.e.* very much in the center of the mass region for which the $b\bar{b}$ mode ϕ^0 studies were performed. For $m_t \sim 200$ GeV, the constant mass value is somewhat larger, in the vicinity of 130 GeV. The behavior of the h^0 and H^0 squared couplings to $b\bar{b}$ and $t\bar{t}$, relative to the ϕ^0, as a function of m_{A^0} is illustrated in Fig. 1. We see that at low m_{A^0} the couplings of the H^0 are fairly SM-like, while after the crossing over (at $m_{A^0} \sim 100 - 130$ GeV) it is the h^0 which has SM-like couplings. Thus, whichever Higgs has mass in the vicinity of m_Z (plus radiative corrections) is roughly SM-like.

However, the $b\bar{b}$ coupling for the Higgs with mass near m_Z is not precisely the same as for the ϕ^0. For $m_{A^0} \gtrsim 50$ GeV it is somewhat larger. This has the useful consequence that the $b\bar{b}$ branching ratios for the H^0 or h^0 can be nearer to 100% than for a ϕ^0 of the same mass. Space does not allow a detailed exposition on the branching ratios of the h^0 and H^0. These are well-known.[1,8] In general, $BR(h^0 \to b\bar{b})$ is very near 1 until m_{ϕ^0} becomes very close to its maximum value (at large m_{A^0}) at which point $BR(h^0 \to b\bar{b})$ declines somewhat as other modes enter the picture. The behavior of $BR(H^0 \to b\bar{b})$ as a function of m_{A^0} is much more complicated and is highly dependent upon $\tan\beta$. In particular, $H^0 \to h^0h^0$ severely suppresses the $H^0 \to b\bar{b}$ branching ratio for much of the relevant m_{A^0} range when $\tan\beta$ is ~ 2. For larger $\tan\beta$, there is a window of moderate m_{A^0} for which $BR(H^0 \to b\bar{b})$

‡ The precise number depends upon $\tan\beta$.

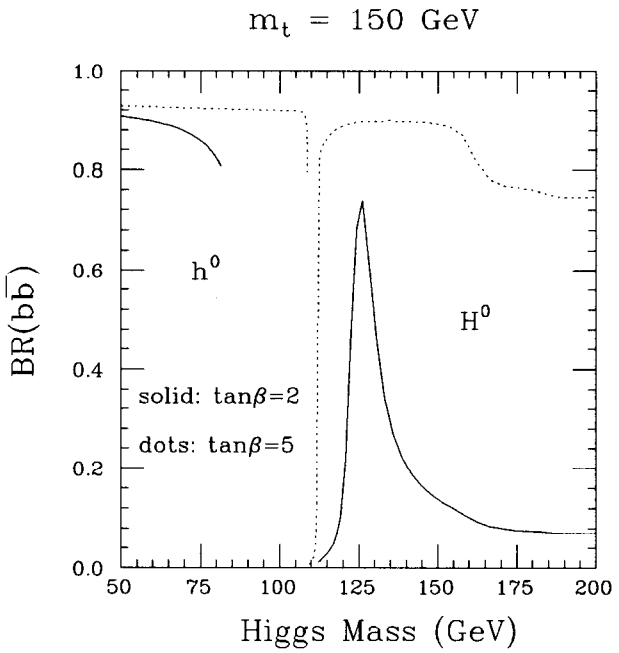

Figure 2: $BR(h \to b\bar{b})$ ($h = h^0$ or H^0) as a function of m_h at $m_t = 150$ GeV, for $\tan\beta = 2$ and 5. We have taken $M_{\tilde{t}} = 1$ TeV. Decays to chargino and neutralino pair states are assumed to be forbidden.

is large. To illustrate, in Fig. 2 we plot $BR(h \to b\bar{b})$ as a function of m_h ($h = h^0$ or H^0) for $m_t = 150$ GeV, and $\tan\beta = 2$ and 5.

2. Results and Discussion

Results for the SSC are displayed in Figs. 3 and 4, for $m_t = 150$ and 200 GeV, respectively. These figures display the regions of m_{A^0}–$\tan\beta$ parameter space where detection of $t\bar{t}h$ with $h \to b\bar{b}$ is possible at the 4σ level for an integrated luminosity of $L = 30$ fb^{-1} — the region of viability for $h = h^0$ is indicated by the letter i), while that for $h = H^0$ is indicated by h). The viable regions for an assortment of several other Higgs signals are also given in each case. The power of the $t\bar{t}b\bar{b}$ final state modes is immediately apparent.

In the case of $m_t = 150$ GeV, Fig. 3, the h^0 (i) and H^0 (h) $t\bar{t}b\bar{b}$ modes are viable in nearly all of parameter space above $m_{A^0} \sim 50$ GeV. The only exception is the delicate cross-over point discussed in the previous section of the paper, where the H^0 and h^0 switch roles. For $m_t = 150$ GeV the critical region is $m_{A^0} \sim 100 - 110$ GeV. For such m_{A^0} values neither the H^0 nor the h^0 has full SM-strength $t\bar{t}$ coupling (see Fig. 1) and, strictly speaking, neither satisfies the 4σ discovery criterion. However, it should be noted that for large $\tan\beta$ the H^0 and h^0 are nearly degenerate at the switch-over. Consequently, their mass peaks can be effectively lumped together, and the gap between the H^0 and h^0 regions is in reality not present for $\tan\beta \gtrsim 10$. The other curves given in Fig. 3 serve primarily to define the window (referred to in our introductory discussion), marked with a large $\times$, for which detection of a MSSM Higgs boson at LEP-II or the SSC was previously deemed to be quite difficult. We

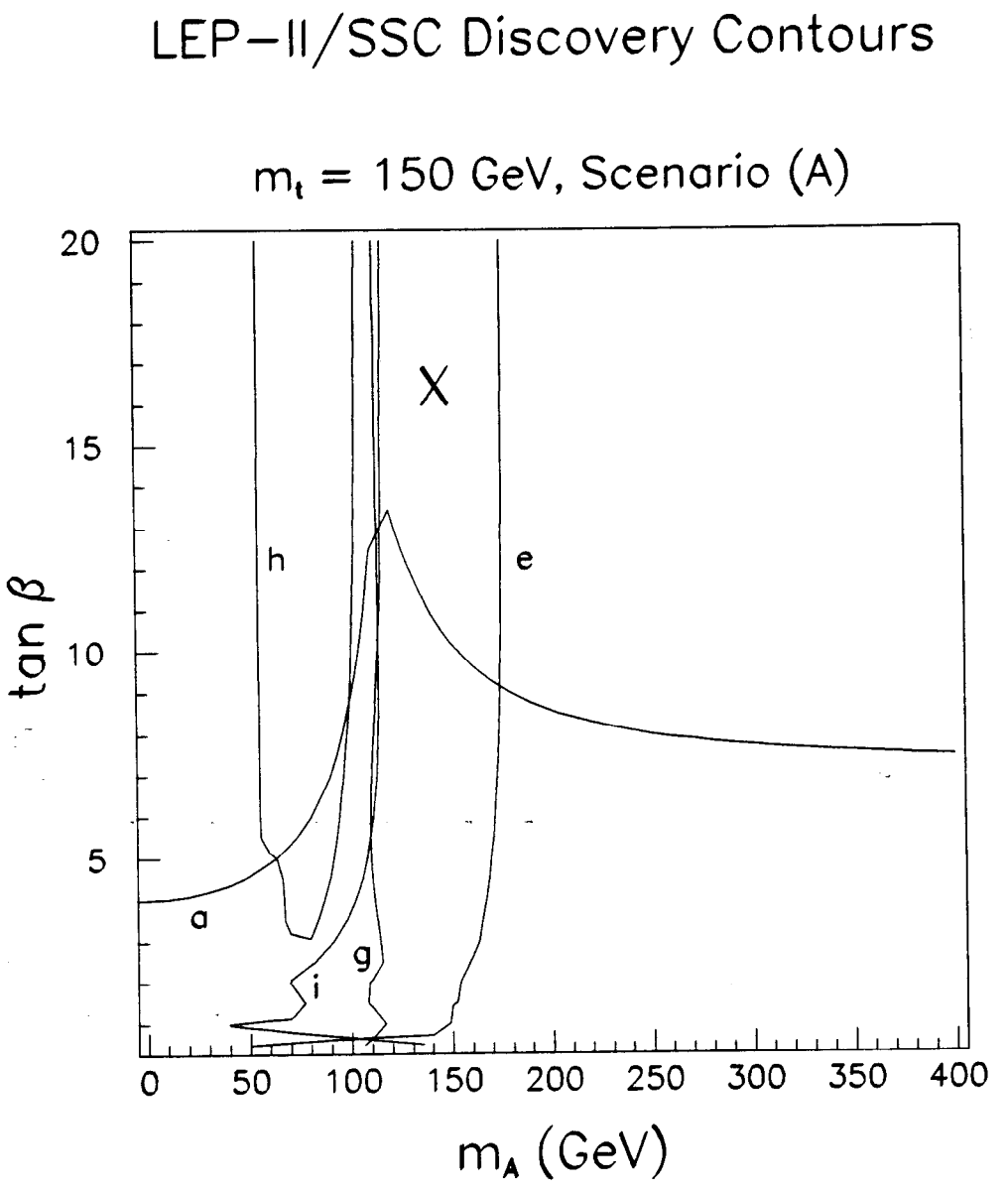

Figure 3: Discovery contours (at the 4σ level) in m_{A^0}–$\tan\beta$ parameter space for the SSC with $L = 30$ fb^{-1} and LEP-200 with $L = 500$ pb^{-1} for the reactions: a) $e^+e^- \to h^0Z$ at LEP-200; e) $Wh^0X \to l\gamma\gamma X$; g) $t \to H^+b$; h) $t\bar{t}H^0$, with $H^0 \to b\bar{b}$; and i) $t\bar{t}h^0$, with $h^0 \to b\bar{b}$. The contour corresponding to a given reaction is labelled by the letter assigned to the reaction above. In each case, the letter appears on the side of the contour for which detection of the particular reaction *is* possible. The letter assignments are chosen to be consistent with those in J. Gunion and L. Orr, Ref. 1, and Refs. 2 and 9, in order to facilitate comparison with earlier results. The large × indicates the location of the window where no MSSM Higgs could be discovered at LEP-II or the SSC without processes h) and i). We have taken $m_t = 150$ GeV, $M_{\tilde{t}} = 1$ TeV and neglected squark mixing. Scenario (A) refers to the notation established in Ref. 9; it corresponds to the case in which charginos and neutralinos are taken to be heavy.

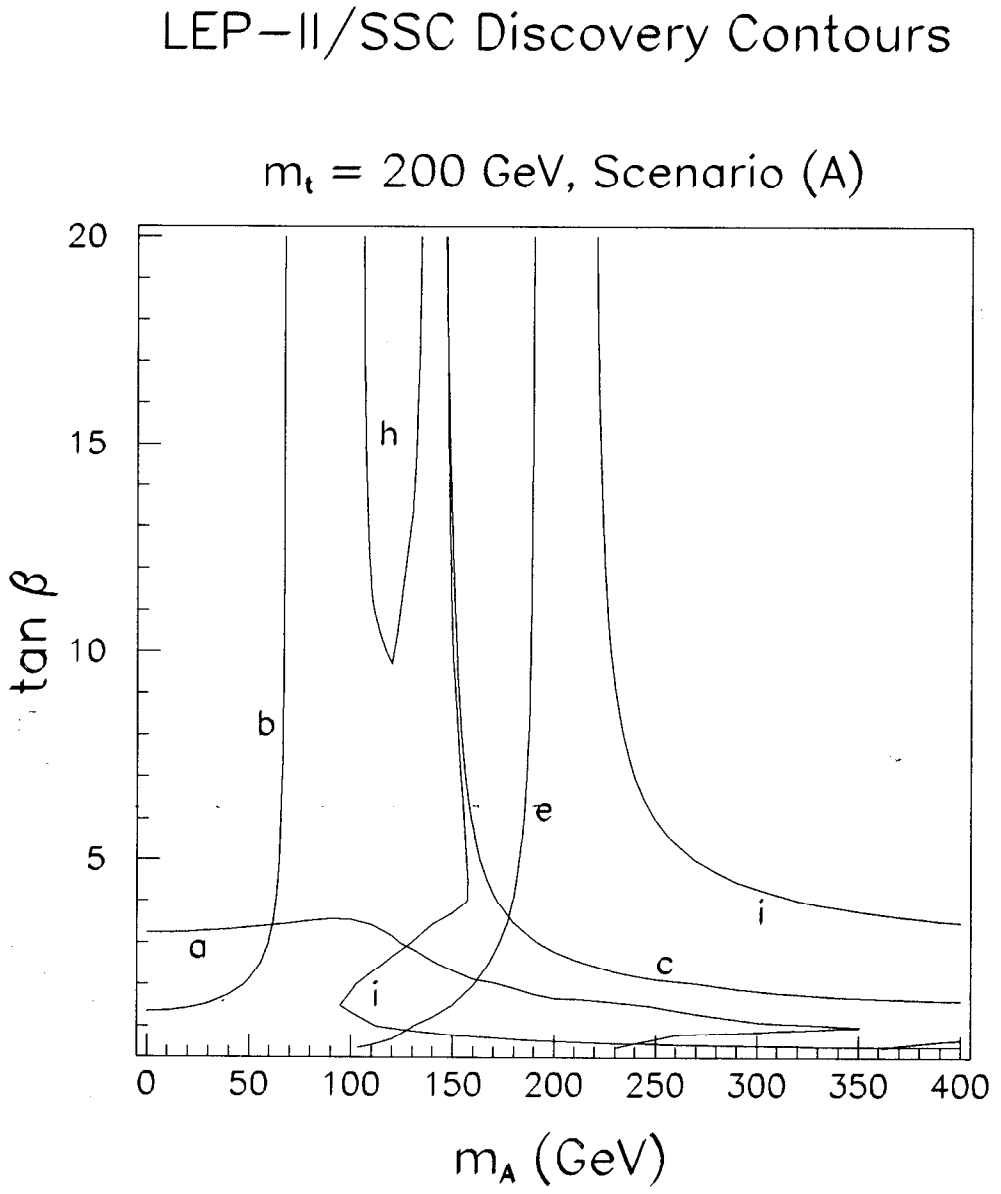

Figure 4: Discovery contours (at the 4σ level) in m_{A^0}–$\tan\beta$ parameter space for the SSC with $L = 30$ fb^{-1} and LEP-200 with $L = 500$ pb^{-1} for the reactions: a) $e^+e^- \to h^0Z$ at LEP-200; b) $e^+e^- \to h^0A^0$ at LEP-200; c) $h^0 \to 4l$; e) $Wh^0X \to l\gamma\gamma X$; h) $t\bar{t}H^0$, with $H^0 \to b\bar{b}$; and i) $t\bar{t}h^0$, with $h^0 \to b\bar{b}$. Conventions as in Fig. 3, except that $m_t = 200$ GeV.

see that the $t\bar{t}h^0$, $h^0 \to b\bar{b}$ mode is viable throughout this window region. In addition, we observe that if the LEP-II Zh^0 detection mode is removed, all but a tiny sliver of parameter space is covered by the $t\bar{t}b\bar{b}$ mode of the h^0 or else by the $t \to H^+b$ mode for H^+ detection.

In addition, everywhere that h^0 detection in the $l\gamma\gamma X$ final states (arising from Wh^0X final states in which $W \to l\nu$ and $h^0 \to \gamma\gamma$) is possible, h^0 detection in the $t\bar{t}b\bar{b}$ final state is also possible.

At $m_t = 200$ GeV (Fig. 4), the $t\bar{t}b\bar{b}$ mode does not cover as large a fraction of parameter space. This is because the h^0 is substantially heavier when m_{A^0} and $\tan\beta$ are both large ($m_{h^0} \gtrsim 130$ GeV), than in the $m_t = 150$ GeV case. Thus, $BR(h^0 \to b\bar{b})$ declines at large m_{A^0} (see Fig. 2) due to the onset of WW^* and ZZ^* channels, while the $t\bar{t}h^0$ cross section is also somewhat smaller. However, there is no window of concern in this case; detection of at least one MSSM Higgs boson is possible throughout all of parameter space even without using the $t\bar{t}b\bar{b}$ modes. In Fig. 4, we have chosen to plot only those modes that allow detection of the h^0 (in particular, $t \to H^+b$ and $H^0 \to 4\ell$ modes are not displayed) in addition to the $t\bar{t}b\bar{b}$ modes for the h^0 and H^0. This figure illustrates the substantial overlap among different h^0 detection modes. In particular, where modes c), e) and i) overlap, we should be able to experimentally verify the relative strengths of the ZZh^0, $t\bar{t}h^0$ and $b\bar{b}h^0$ couplings. In addition, we see that the h^0 can be discovered, either at LEP-II or the SSC for all but a window of parameter space with $\tan\beta \gtrsim 3.5$ and $70 \lesssim m_{A^0} \lesssim 150$ GeV.

For smaller values of m_t, *e.g.* in the vicinity of 100 GeV, the $t\bar{t}b\bar{b}$ detection mode for the h^0 remains viable over much the same region of parameter space as illustrated in Fig. 3 for $m_t = 150$ GeV. This is because radiative corrections to the h^0 mass are small, and the upper limit for m_{h^0} (reached for $m_{A^0} \gtrsim 100$ GeV) lies between ~ 50 GeV and m_Z for $\tan\beta$ between 2 and ∞. Thus, despite the increase of $t\bar{t}$-related backgrounds relative to those found for $m_t = 150$ GeV *at any given Higgs mass*, m_{h^0} moves into a lower mass region where these backgrounds are actually smaller and the statistical significances (for 100% $b\bar{b}$ branching ratio) quoted earlier are larger. The region of viability for the H^0, whose mass remains in the vicinity of m_Z for $m_{A^0} \lesssim 100$ GeV, does decrease somewhat at $m_t = 100$ GeV relative to $m_t = 150$ GeV because of the increased $t\bar{t}$-related background levels. Further details will be given in a longer paper.[10] Of course, current indications from both the Tevatron and LEP are that m_t is very likely to be $\gtrsim 130 - 140$ GeV. If m_t were to turn out to be near 100 GeV, the h^0 mass is sufficiently small that LEP-II will have an excellent chance of detecting it in any case.

For $L = 100$ fb^{-1}, the LHC is roughly equivalent to the SSC at $L = 30$ fb^{-1}, assuming the same efficiency and purity of b-tagging. However, the efficiency of b-tagging at the LHC, given the many overlapping events expected, may not be as great as assumed here. Other experimental problems could arise regarding overlapping jets.

In the above, we have ignored the CP-odd A^0. This is because for both $m_t = 150$ and 200 GeV (and for $\tan\beta \gtrsim 0.5$) detection of the A^0 in the $t\bar{t}b\bar{b}$ mode is confined to a small area with $\tan\beta \lesssim 2$ and m_{A^0} below roughly 130 GeV. The upper limit is given by the onset of the $A^0 \to Zh^0$ decay mode. Exactly how low we can go in m_{A^0} at low $\tan\beta$ values is not currently known. We estimate that the results of Ref. 6 can be safely extrapolated down to 50-60 GeV. But extension below that would require more detailed study. The inability to detect the A^0 for $\tan\beta \gtrsim 2$ is simply a consequence of the fact that the $A^0t\bar{t}$ coupling is

suppressed by $1/\tan\beta$. Thus, by $\tan\beta = 2$ the $A^0 t\bar{t}$ cross section is at most 1/4 of SM size.*

Of course, in this letter we have focused on the case where supersymmetric partner masses are assumed to be large. The results for the $t\bar{t}b\bar{b}$ discovery modes of the h^0 and H^0 are essentially unmodified unless the chargino and/or neutralino masses lie below 50-60 GeV. This is because the $t\bar{t}b\bar{b}$ mode is mainly viable for regions of parameter space such that the Higgs (h^0 or H^0) mass is of order 80-130 GeV. If the squark mass is also taken to be light, then the region of viability for the $t\bar{t}b\bar{b}$ mode at $m_t = 200$ GeV actually expands since the h^0 has mass $\lesssim m_Z$, and thus will have nearly 100% branching ratio to $b\bar{b}$, as well as being in the mass region of maximal sensitivity for the $t\bar{t}b\bar{b}$ mode. Of course, other SM final state detection modes do suffer if neutralinos and/or charginos are light. As detailed in Ref. 9, the $H^0 \to 4\ell$ mode is especially vulnerable. The power of the $t\bar{t}b\bar{b}$ detection modes, however, is such that the SSC alone remains able to see at least one MSSM Higgs boson throughout essentially all of MSSM parameter space.

3. Conclusion

We have demonstrated that b-tagging can be used to isolate $t\bar{t}h$ events, in which $h \to b\bar{b}$, for $h = h^0$ or H^0 over a substantial range of the parameter space of the Minimal Supersymmetric Model. With inclusion of this detection mode, for an accumulated luminosity of $L = 30$ fb^{-1} the SSC alone is guaranteed to find at least one (and more probably several) of the MSSM Higgs bosons, for any value of $m_t \gtrsim 140$ GeV.

4. Acknowledgements

This work has been supported in part by Department of Energy grants #DE-FG03-91ER40674 and #DE-AC03-76SF00515, by Texas National Research Laboratory grants #RGFY93-330 and #RCFY93-229, and by National Science Foundation grant NSF-PHY-88-18535. JFG would like to thank L. Orr and H.E. Haber, with whom some of the underlying programs employed for this project were developed.

References

1. J.F. Gunion and L.H. Orr, *Phys. Rev.* **D46** (1992) 2052. Z. Kunszt and F. Zwirner, *Nucl. Phys.* **B385** (1992) 3. H. Baer, M. Bisset, C. Kao and X. Tata, *Phys. Rev.* **D46** (1992) 1067. V. Barger, K. Cheung, R.J.N. Phillips and A.L. Stange, *Phys. Rev.* **D46** (1992) 4914.
2. For a review see J.F. Gunion, preprint UCD-92-20, to appear in *Perspectives in Higgs Physics*, ed. G. Kane, World Scientific Publishing (1992).
3. For a review, see H.E. Haber, preprint UCSC-92/31, to appear in *Perspectives in Higgs Physics*, ed. G. Kane, World Scientific Publishing (1992).
4. Z. Kunszt and F. Zwirner, Ref. 1.
5. See the LHC detector design studies.

* Actually, the γ_5 coupling also makes the cross section shape different as a function of Higgs mass, so that this scaling argument is not precise.

6. J. Dai, J.F. Gunion, and R. Vega, preprint UCD-93-18 (1993).

7. J.F. Gunion, H.E. Haber, G. Kane and S. Dawson, *The Higgs Hunter's Guide*, Addison-Wesley, Redwood City, CA (1990).

8. R. Bork, J.F. Gunion, H.E. Haber, A. Seiden, *Phys. Rev.* **D46** (1992) 2040. J.F. Gunion, H.E. Haber, and C. Kao, *Phys. Rev.* **D46** (1992) 2907. V. Barger, M.S. Berger, A.L. Stange, and R.J.N. Phillips, *Phys. Rev.* **D45** (1992) 4128.

9. J.F. Gunion, preprint UCD-93-8 (1993), to appear in the Proceedings of *Properties of SUSY Particles*, INFN workshop, eds. L. Cifarelli and A. Zichichi, Erice, Sicily, October (1992).

10. J. Dai, J.F. Gunion and R. Vega, work in progress.